

Heptad Repeats Regulate Protein Phosphatase 2A Recruitment to I- κ B Kinase γ /NF- κ B Essential Modulator and Are Targeted by Human T-lymphotropic Virus Type 1 Tax*

Received for publication, November 7, 2006, and in revised form, January 16, 2007. Published, JBC Papers in Press, February 21, 2007, DOI 10.1074/jbc.M610392200

Sohee Hong[‡], Ling-Chi Wang^{§1}, Xiang Gao[‡], Yu-Liang Kuo[‡], Baoying Liu[‡], Randall Merling[‡], Hsing-Jien Kung^{¶1}, Hsiu-Ming Shih^{§1}, and Chou-Zen Giam^{‡2}

From the [‡]Department of Microbiology and Immunology, Uniformed Services University of the Health Sciences, Bethesda, Maryland 20814, the [§]Division of Molecular and Genomic Medicine, National Health Research Institutes, 128, Sec 2, Yen-Chiu-Yuan Road, Taipei 115, Taiwan, and the [¶]University of California Davis Cancer Center, Sacramento, California 95817

The switching on-and-off of I- κ B kinase (IKK) and NF- κ B occurs rapidly after signaling. How activated IKK becomes down-regulated is not well understood. Here we show that following tumor necrosis factor- α stimulation, protein phosphatase 2A (PP2A) association with IKK is increased. A heptad repeat in IKK γ , helix 2 (HLX2), mediates PP2A recruitment. Two other heptad repeats downstream of HLX2, termed coiled-coil region 2 (CCR2) and leucine zipper (LZ), bind HLX2 and negatively regulate HLX2 interaction with PP2A. HTLV-1 transactivator Tax also binds HLX2, and this interaction is enhanced by CCR2 but reduced by LZ. In the presence of Tax, PP2A-IKK γ binding is greatly strengthened. Interestingly, peptides spanning CCR2 and/or LZ disrupt IKK γ -Tax and IKK γ -PP2A interactions and potentially inhibit NF- κ B activation by Tax and tumor necrosis factor- α . We propose that when IKK is resting, HLX2, CCR2, and LZ form a helical bundle in which HLX2 is sequestered. The HLX2-CCR2-LZ bundle becomes unfolded by signal-induced modifications of IKK γ or after Tax binding. In this conformation, IKK becomes activated. IKK γ then recruits PP2A via the exposed HLX2 domain for rapid down-regulation of IKK. Tax-PP2A interaction, however, renders PP2A inactive, thus maintaining Tax-PP2A-IKK in an active state. Finally, CCR2 and LZ possibly inhibit IKK activation by stabilizing the HLX2-CCR2-LZ bundle.

The kinetics of the NF- κ B regulatory pathway, from its activation to its return to the resting state, is rapid. Within minutes after treatment with inducers such as interleukin-1, tumor necrosis factor- α (TNF- α)³, or bacterial lipopolysaccharide,

I- κ B kinase (IKK) is activated. I- κ B α and I- κ B β in turn become serine-phosphorylated by IKK and are targeted for polyubiquitination and degradation by proteasome (for a recent review, see Ref. 1). This leads to nuclear accumulation of NF- κ B and activation of mRNA transcription of a large array of cellular genes, including that of I- κ B α . The surge in mRNA and protein synthesis of I- κ B α is then accompanied by its transport to the nucleus and the redistribution of NF- κ B/I- κ B α complex back to the cytoplasm (1, 2). Recent studies have indicated that IKK activity peaks at 10 min and declines to 25% of peak activity at 30 min post-TNF- α induction (3, 4). Coincident with the rapid rise and fall of IKK activity, I- κ B α level becomes undetectable due to IKK phosphorylation and proteasome degradation at 20 min and reappears at 40 min post-induction as a consequence of *de novo* synthesis (3, 4).

The core IKK consists of two highly homologous catalytic subunits α and β of 85 and 87 kDa in sizes, respectively, and a 48-kDa regulatory subunit, IKK γ /NF- κ B essential modulator (NEMO, referred to as IKK γ herein) (5, 6). Both IKK α and IKK β contain NH₂-terminal kinase domains followed by leucine zippers (LZ) and helix-loop-helix domains that mediate protein-protein interactions important for IKK oligomerization and kinase activity (6, 7). IKK γ also contains extensive helical regions and leucine zipper domains that are involved in protein-protein interaction (5, 6). *In vivo*, the IKK holoenzyme exists as a large protein complex of at least 700–900 kDa in size (6, 7). It is not clear what other protein components are present in the holo-IKK enzyme complex in addition to IKK α , IKK β , and IKK γ (6). It has been proposed that the stoichiometry of IKK holoenzyme is $\alpha_1\beta_1\gamma_2$ or $\beta_2\gamma_2$, with each IKK holoenzyme containing two IKK γ subunits (8). Finally, tetramerization of IKK γ has also been reported to be important for IKK activation (9).

Activation of IKK requires serine phosphorylation of its activation loop by autophosphorylation and/or by upstream kinases such as MEKK and TAK1 (1, 6, 10, 11). Polyubiquitination of IKK γ /NF- κ B essential modulator by the ubiquitin ligase, TRAF6, also plays a critical role in initiating IKK activation (12, 13). TRAF6 acts upstream of TAK1 and may be responsible for TAK1 recruitment to IKK (12, 13). Although the mechanisms for IKK activation have been extensively studied, the molecular events that control rapid IKK down-regulation are not well

* This work was supported by grants from the National Institutes of Health and a grant from the United States Military Cancer Institute (to C.-Z. G.). The costs of publication of this article were defrayed in part by the payment of page charges. This article must therefore be hereby marked "advertisement" in accordance with 18 U.S.C. Section 1734 solely to indicate this fact.

¹ Present address: Institute of Biomedical Sciences, Academia Sinica, 128, Sec 2, Yen-Chiu-Yuan Road, Taipei 115, Taiwan.

² To whom correspondence should be addressed: Dept. of Microbiology and Immunology, Uniformed Services University of the Health Sciences, 4301 Jones Bridge Rd., Bethesda, MD 20814. Tel.: 301-295-9624; Fax: 301-295-1545; E-mail: cgiam@usuhs.mil.

³ The abbreviations used are: TNF- α , tumor necrosis factor- α ; HTLV-1, human T-lymphotropic virus type 1; IKK, I- κ B kinase; PP2A, protein phosphatase 2A; CCR, coiled-coil region; LZ, leucine zipper; HA, hemagglutinin; HEK, human embryonic kidney; GST, glutathione S-transferase.

IKK γ Is a Molecular Switch

understood. Many lines of evidence suggest that the major serine/threonine protein phosphatase, PP2A, is involved (14–16).

HTLV-1 Tax activates IKK constitutively (17–22). This is due in part to a direct interaction between Tax and IKK γ (20, 22, 24). While IKK γ is essential for IKK activation, the mechanism through which IKK γ controls IKK activity remains unclear. We have shown that via a tripartite interaction, Tax, PP2A, and IKK γ form a stable ternary complex, wherein PP2A activity is inhibited or diminished due to its interaction with Tax (16). In essence, IKK is activated by serine phosphorylation upon extracellular stimulation. Phospho-IKK then becomes rapidly inactivated by IKK γ -associated PP2A, returning it to the resting state. These results suggest that in HTLV-1 infected or transformed cells, PP2A inhibition by IKK γ -bound Tax maintains IKK in an active, phosphorylated state, causing constitutive phosphorylation and degradation of I- κ B (16).

IKK γ contains multiple α -helical heptad repeats that include HLX1 (helix-loop-helix 1), CCR1 (coiled-coil region 1), HLX2, CCR2, and LZ (leucine zipper). HLX1 and CCR1 regions are important for IKK γ interaction with IKK α and IKK β (25, 26). In this study, the protein-protein interaction of IKK γ , PP2A, and Tax is investigated. We have localized HLX2 heptad repeat of IKK γ to be the primary binding domain of PP2A and Tax and have shown additionally that HLX2, CCR2, and LZ interact with one another dynamically to modulate PP2A recruitment and Tax interaction. Our results suggest that the structures of HLX2, CCR2, and LZ possibly alternate between a helical bundle (closed/inactive conformation) and an extended α -helix (open/active conformation) to regulate the accessibility of HLX2 to PP2A. Tax, through its interaction with HLX2 and CCR2, maintains IKK γ in an open/active conformation. Although this structure avidly recruits PP2A, the latter is inhibited by Tax, thereby keeping IKK constitutively active. CCR2 and LZ peptides possibly stabilize the HLX2-CCR2-LZ bundle, thereby keeping IKK γ in a closed conformation and preventing PP2A and Tax from binding IKK γ . These data indicate that the dynamic interaction of HLX2-CCR2-LZ heptad repeats modulates the recruitment of PP2A and allows IKK γ to function as a molecular switch that can turn IKK on or off rapidly. HTLV-1 Tax interaction with IKK γ and PP2A keeps the switch at the “on” position and IKK constitutively active.

EXPERIMENTAL PROCEDURES

Yeast Two- and Three-hybrid Assays and β -Galactosidase Assay—Yeast two-hybrid assays were performed in strain L40 (*MATa*, *his3 Δ 200*, *trp1-901*, *leu2-3112*, *ade2*, *LYS2::lexA-HIS3*, *URA3::lexA-lacZ*) where LacZ and HIS3 are driven by minimal GAL1 promoters fused to eight and four *lexA* boxes, respectively (27). A 2- μ plasmid, BTM116 (TRP), containing the LexA DNA-binding domain (27) was used to produce LexA-IKK γ fusions. The coding sequences for full-length IKK γ and truncated variants were generated using standard PCR methods. Specific information concerning the oligonucleotide sequence is available upon request. Constructs were ligated into the EcoRI insertion site of pBTM116. VP16-PP2A (LEU) contains PP2A $_c$ - α cDNA sequence in a 1-kB NcoI (blunt-ended) and EcoRI fragment joined to the VP16 activation domain via NotI (blunt-ended) and EcoRI sites. VP16-Tax was similarly constructed. The coding sequences for CCR2 (IKK γ

250–307), LZ (IKK γ 300–360), and CCR2-LZ (IKK γ 250–360) were generated by PCR using appropriate oligonucleotides and fused to the VP16 activation domain via EcoRI and BamHI sites. Specific information concerning the oligonucleotide sequence is available upon request. For the yeast three-hybrid assays, *tax* cDNA was placed under the control of the Met-25 promoter on HO-pMET-poly-KanMX4-HO vector (28) and integrated at the mating type locus after transformation. The activities of β -galactosidase were measured using an “enhanced β -galactosidase assay kit (CPRG)” purchased from Gene Therapy Systems (San Diego, CA) as prescribed by the vendor and normalized against the absorbance unit of each culture. Relative β -galactosidase activities are plotted.

Antibodies—Mouse hybridoma antibody 4C5 reacts with amino acid residues 333–353 of Tax.⁴ Anti-PP2A C subunit monoclonal antibody reacts with the COOH-terminal amino acid residues 295–309 of the catalytic subunit of human PP2A and was from Santa Cruz Biotechnology, Inc., as well as antibodies against PP2A A subunit, actin, VP16, IKK β , and IKK γ . Antibodies against HA, KT3, and EE epitopes were obtained from Covance Inc.

Glutathione S-transferase Pulldown Assays—For production of GST-IKK γ fusion proteins, the coding sequences for full-length IKK γ and truncated variants were generated using standard PCR methods as above. Constructs were ligated into the NcoI/EcoRI insertion site of pGEX-2T. Bacterial lysis, recombinant protein purification, and binding to glutathione beads was done as described previously (16).

For GST pulldown experiments, 500 ng each of purified GST, GST-IKK γ , or GST-IKK γ truncated variants were incubated for 30 min at 30 °C with 1.0 ml of cell lysate from 293T cells transfected with the EE-PP2A A α expression plasmid. Cell lysate was prepared by incubating $\sim 7 \times 10^6$ cells with 1 ml of a buffer solution containing 25 mM HEPES (pH 7.9), 5 mM KCl, 0.5 mM MgCl₂, 0.5 mM EDTA, 1 mg/ml bovine serum albumin, 10% glycerol, 0.15% Nonidet P-40, 0.25 mM dithiothreitol, and 0.5 mM phenylmethylsulfonyl fluoride. Incubation of the lysate with the beads, washing, and subsequent immunoblots were done as reported previously (16), except that 120 μ l of a 50% slurry of prewashed glutathione-Sepharose 4B was added to each binding reaction.

S-Agarose PullDown—Human embryonic kidney (HEK) 293T cells were transfected with one or more of the following constructs: H6/S-PP2A α , EE-PP2A α , HA-IKK γ , and PP2A α . PCR was used to generate the hexa-histidine and RNase S-peptide-tagged (H6/S)-PP2A α cDNA, which was ligated into the EcoRI/NotI insertion site of pTriEx-4Neo. Cell lysates from the transfected 293T cells were used for the S-agarose pulldown assay. Lysis buffer contained 50 mM Tris (pH 7.5), 150 mM NaCl, 10 mM EDTA, 1% Triton X-100, and complete protease inhibitor mixture (as prescribed by Roche Applied Science). Cell lysate, obtained by incubating 7×10^6 cells with 1 ml of lysis buffer, was mixed with 0.2 ml of S-protein-agarose beads (Novagen) at 4 °C for 2 h. Beads from each sample were washed four times with a buffer solution contain-

⁴ S. Hong, L.-C. Wang, X. Gao, Y.-L. Kuo, B. Liu, R. Merling, H.-J. Kung, H.-M. Shih, and C.-Z. Giam, unpublished results.

ing 20 mM Tris-HCl (pH 7.5), 150 mM NaCl, 0.1% Triton X-100, then boiled for 7 min with SDS-PAGE sample buffer and analyzed by immunoblotting as described previously (16).

Co-immunoprecipitation—For IKK γ -HA immunoprecipitation, transfected 293T cells were harvested and washed twice with cold PBS, lysed with 1 ml of lysis buffer containing 50 mM Tris (pH 7.5), 150 mM NaCl, 10 mM EDTA, 1% Triton X-100, and complete protease inhibitor mixture (Roche Applied Science), and incubated on ice for 15 min. Cell debris was removed by centrifugation at 12,000 rpm for 15 min at 4 °C. Lysates were precleared by incubation with 20 μ l of 50% slurry of protein G-agarose (Sigma) for 1 h at 4 °C. Cell lysates were clarified by centrifugation at 12,000 rpm for 30 min at 4 °C. Anti-HA-agarose (Covance) was mixed with the precleared cell lysates and incubated at 4 °C for 2 h. The reaction

mixtures were then washed three times with cold lysis buffer, boiled for 7 min with SDS-PAGE sample buffer, and analyzed by immunoblots as described (16). The IKK γ immunoprecipitation was done similarly, except that IKK γ antibody was used. Immunoprecipitation of whole cell lysates prepared from Jurkat and MT4 cells was similar as above except an anti-PP2A A subunit antibody and 10⁷ cells each were used; and the lysis buffer contained only 0.1% Triton X-100.

DNA Transfection, TNF- α Induction, and Luciferase Reporter Assay—The coding sequences for influenza HA-VP16 activation-domain fusion (HAVP), HAVP-CCR2, HAVP-LZ, and HAVP-CCR2-LZ were generated by PCR and ligated into the EcoRI/BamHI insertion site of pcDNA 3.1. HEK293T cells were seeded in 24-well plates (2.5 \times 10⁴ cells/well) and transfected using the calcium phosphate (Invitrogen) method with 1 μ g of E-selectin-luciferase reporter, 0.5 μ g of pRL-TK (*Renilla* luciferase internal control), and the expression plasmid for the respective IKK γ peptides (0.25, 0.5, 1.0, and 2 μ g). The total amount of DNA was normalized by the addition of pcDNA3.1. For TNF- α induction, at 40 h post-transfection, 2 ng/ml human TNF- α (Sigma) was added, and incubation was continued for 8 h. At the end of TNF- α treatment, the recipient cells were lysed with a reporter lysis buffer (luciferase reagent, Promega). Luciferase activity was detected with a luminometer after mixing 10 μ l of extract with 25 μ l of luciferase substrate (Promega). For NF- κ B activation by Tax, 0.5 μ g of Tax expression vector was transfected into 293T cells.

RESULTS

PP2A Associates with Activated IKK—We have shown previously that the catalytic C subunit of PP2A (PP2Ac), Tax, and IKK form a stable ternary complex (16). To investigate the physiological role of PP2A in regulating IKK, we used co-immunoprecipitation to measure their association in the presence or absence of extracellular stimulation. As shown in Fig. 1, only weak IKK-PP2A binding was detectable in 293T cells that were resting (Fig. 1, lane 3). Interestingly, when 293T cells were stimulated with TNF- α , concurrent with IKK activation and I- κ B degradation, PP2A binding to IKK was greatly increased (Fig. 1, lane 4). We interpret these data to suggest that the recruitment of PP2A to IKK is responsible for the rapid down-regulation of IKK following TNF- α signaling.

To determine whether Tax and IKK γ interact with the PP2A holoenzyme, 293T cells were transiently transfected with expression plasmids for HA-tagged IKK γ , EE-tagged PP2A A α (A subunit), and His/S-peptide-tagged PP2A C α (C

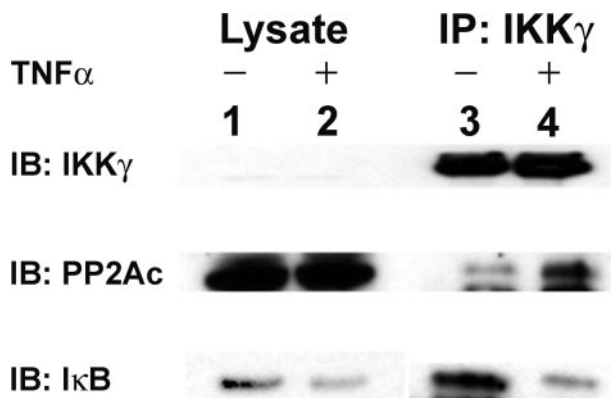


FIGURE 1. **PP2A interacts with activated IKK.** HEK293T cells were treated with TNF- α (10 ng/ml, 15 min) or not. Shown are immunoblots (IB) of whole cell lysates (lanes 1 and 2) or anti-IKK γ immunoprecipitates (IP) (lanes 3 and 4) probed with indicated antibodies.

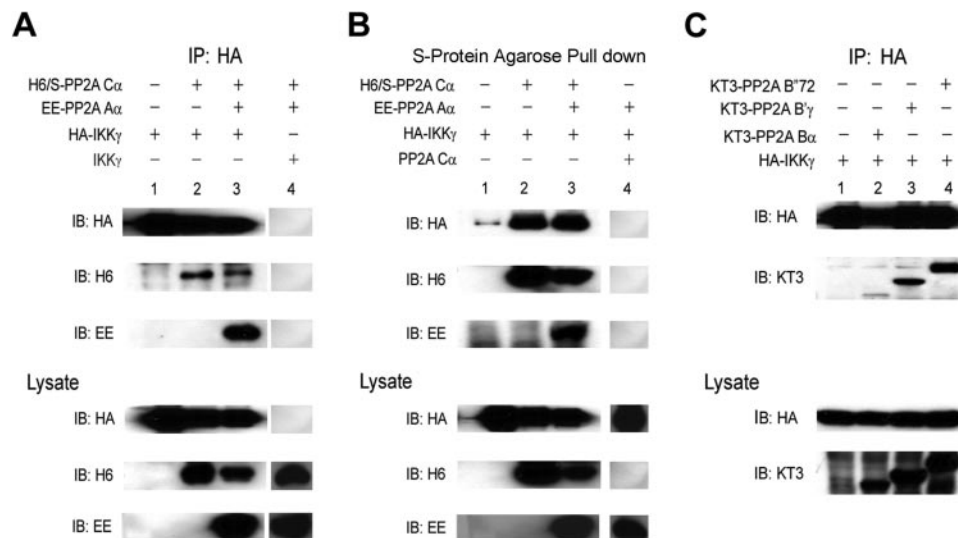


FIGURE 2. **IKK γ interacts with PP2A holoenzyme.** A, immunoblots (IB) of anti-HA-IKK γ immunoprecipitates (IP: HA) (top panel) or corresponding input whole cell lysates (bottom panel) from 293T cells transfected with various combinations of expression plasmids for hexahistidine-S-peptide-tagged PP2AC α subunit (H6/S-PP2AC α), EE-tagged PP2A A α subunit (EE-PP2AA α), and HA-tagged IKK γ (HA-IKK γ) (lanes 1–3). HA-tagged IKK γ was substituted with untagged IKK γ as a control (lane 4). B, immunoblots (IB) of RNase S-protein pull-down (top panel) or corresponding input whole cell lysates (bottom panel) from 293T cells transfected with various combinations of the same plasmids as A, except H6/S-PP2AC α was substituted with untagged PP2AC α in lane 4 as a negative control. C, immunoblots (IB) of anti-HA immunoprecipitates (IP) (top panel) or corresponding whole cell lysates (bottom panel) from 293T cells transfected with expression plasmids for KT3-tagged PP2A B subunits: KT3-PP2AB⁷², KT3-PP2AB^γ, and KT3-PP2AB α , respectively together with an expression plasmid for HA-IKK γ . In all panels the antibodies used in the immunoblots (IB) are indicated.

IKK γ Is a Molecular Switch

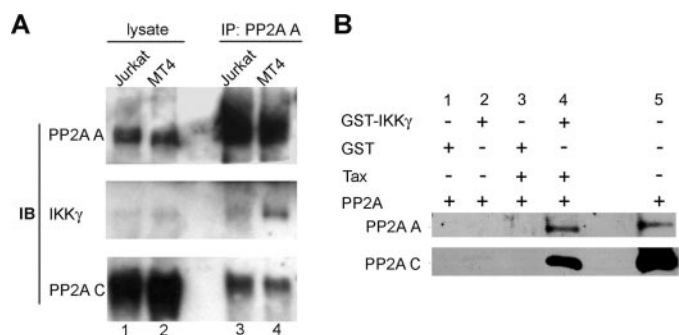


FIGURE 3. Tax increases association of PP2A holoenzyme with IKK γ . *A*, immunoblots (IB) of PP2A A and C subunits and IKK γ . Lanes 1 and 2 represent input lysates of Jurkat (HTLV-1-unrelated) and MT4 (HTLV-1-transformed, Tax-expressing) T cell lines, respectively. Lanes 3 and 4 represent anti-PP2A A immunoprecipitates of Jurkat and MT4, respectively. *B*, GST pull-down was carried out as described previously (16). Purified GST and GST-IKK γ (were incubated with purified PP2A (comprising largely of A and C subunits, lane 5) in the presence or absence of bacterially derived Tax purified on nickel-nitrilotriacetic acid-Sepharose via a COOH-terminal hexahistidine tag.

subunit) in different combinations. Co-immunoprecipitation with HA antibody indicated that both PP2A α and PP2A β interact with IKK γ (Fig. 2*A*). Likewise, pull down of PP2A C α using agarose beads conjugated with RNase-S-protein showed that PP2A C α interacted with both IKK γ and PP2A A α (Fig. 2*B*). As might be expected, IKK β was also detected in the pull-down of PP2A C α .⁴

We next examined interactions between PP2A B subunits and IKK γ . Here again, 293T cells were transiently transfected with expression plasmids for HA-IKK γ and each of three KT3-tagged PP2A B subunits: B α , B' γ , and B''72, respectively. Immunoprecipitation with HA antibody indicated that IKK γ associated with all three B subunits (Fig. 2*C*). This suggests that IKK γ probably interacts with multiple isoforms of PP2A holoenzyme containing different B subunits and is consistent with previous data showing the C subunit to be the direct mediator of the interaction.

To confirm a direct interaction between PP2A holoenzyme with IKK γ *in vivo*, immunoprecipitation was carried out for cell lysates derived from an HTLV-1-transformed T cell line, MT4, and an HTLV-1-unrelated T cell line, Jurkat, using the PP2A A subunit antibody. As expected, PP2A A antibody co-precipitated both the PP2A A and C subunits (Fig. 3*A*, lanes 3 and 4). Importantly, IKK γ also co-precipitated with the PP2A A subunit (Fig. 3*A*, lanes 3 and 4). Consistent with the notion that PP2A binding to IKK becomes increased in the presence of Tax, a higher level of IKK γ was found to associate with PP2A in the MT4 cell lysate (compare Fig. 3*A*, lanes 3 and 4). Finally, purified PP2A enzyme comprising largely of A and C subunits (from Upstate Biotechnology Inc.; Fig. 3*B*, lane 5) was mixed with GST-IKK γ or GST in the presence or absence of purified, bacterially derived Tax protein (16) and incubated with glutathione-agarose beads to pull down GST-IKK γ or GST and the associated proteins. As shown in Fig. 3*B*, no interaction between PP2A with GST was detectable irrespective of the addition of Tax (lanes 1 and 3). While a weak association between PP2A and GST-IKK γ could be seen (lane 2), a much stronger binding of both PP2A A and C subunits to GST-IKK γ was observed in the presence of Tax. Together, these results

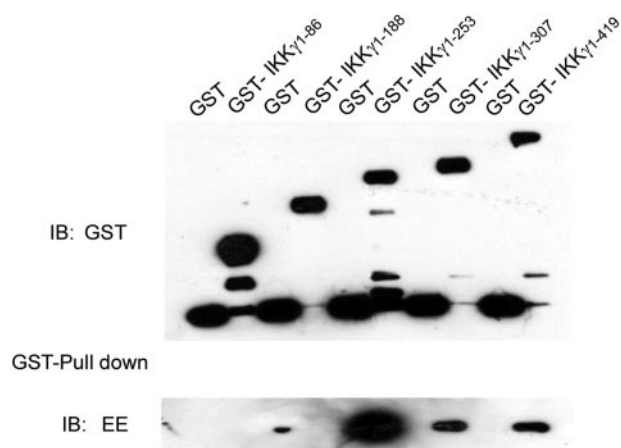


FIGURE 4. PP2A binds the HLX2 heptad repeat of IKK γ . Anti-GST immunoblot (IB) of purified GST and GST fusions containing various IKK γ COOH-terminal truncations (top panel (left to right) IKK γ -1-86, IKK γ -1-188, IKK γ -1-253, and IKK γ -1-307), and full-length IKK γ (IKK γ -1-419). Purified GST and GST fusions were incubated with cell lysate from 293T cells transfected with the EE-PP2A α expression plasmid. Shown is the pull-down immunoblotted with an anti-EE antibody (bottom panel).

support the idea that PP2A holoenzyme becomes recruited to TNF- α -activated or Tax-activated IKK.

The HLX2 Domain of IKK γ Interacts with PP2A—To localize the domain(s) of IKK γ that interacts with PP2A, a series of IKK γ COOH-terminal truncations were made wherein the various helical domains of IKK γ were successively deleted. These truncations were designed based on the paircoil and multicoil programs of Bonnie Berger (29). The deletions were fused with GST to facilitate their purification and analysis. Extracts from 293T cells transiently expressing EE-PP2A A α were then incubated with glutathione-Sepharose beads charged with purified GST-tagged IKK γ -1-86, IKK γ -1-188, IKK γ -1-253, IKK γ -1-307, or full-length IKK γ -1-419. Because PP2A C and A subunits are tightly associated, the capture of EE-PP2A A α by the GST fusions with various IKK γ deletions was used as a surrogate for PP2A binding. Proteins bound to the beads were resolved on 12% SDS-PAGE and immunoblotted with either anti-EE or anti-GST antibody. The pull-down experiment revealed the following order of binding affinities to PP2A A α : IKK γ -1-253 \gg IKK γ -1-307, IKK γ -1-419 \gg IKK γ -1-188. Binding of PP2A to IKK γ -1-86 was not detectable (Fig. 4). Based on this result, we conclude that the primary PP2A-binding site of IKK γ resides in the HLX2 domain, between amino acid residues 188 and 253.

In a complementary approach, the coding sequences of IKK γ deletions and PP2A C α were fused to the LexA DNA-binding domain (BD) and the VP16 activation domain (AD), respectively, and introduced into a *Saccharomyces cerevisiae* reporter strain, L40, for two-hybrid analysis (27, 30). In agreement with the results above that point to the importance of IKK γ -188–253, the two-hybrid system also revealed the affinity of interaction between IKK γ derivatives and PP2A C α in an order similar to the pull-down results, *i.e.* BDIKK γ -1-253 $>$ BDIKK γ -1-307 $>$ BDIKK γ -1-419 \gg BDIKK γ -1-188 and BDIKK γ -151–419 (Fig. 5*A*, solid bars). Neither BDIKK γ -1-86 nor BDIKK γ -151–307 interacted with PP2A C α (Fig. 5*A*, solid bars). Because the protein sequence and overall structure of *S. cerevisiae* and

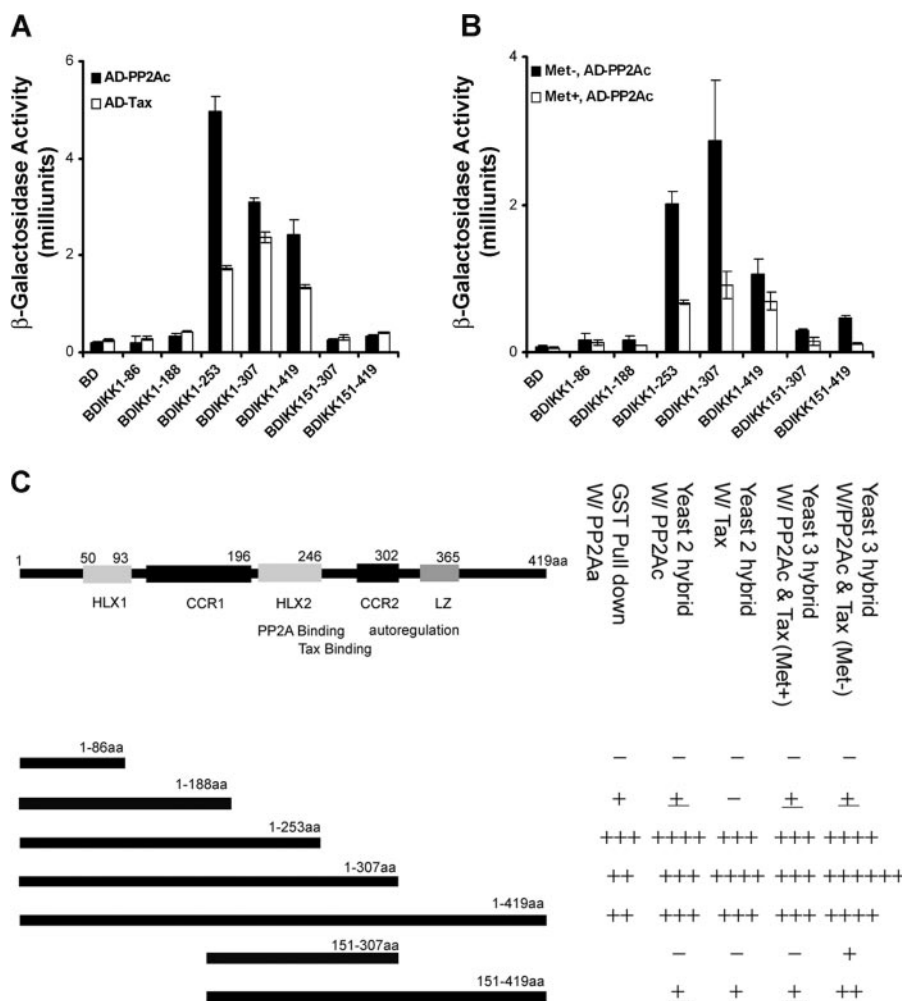


FIGURE 5. Heptad repeats of IKK γ interact with Tax and PP2A. *A*, a yeast two-hybrid assay was used to determine the regions of IKK γ which interact with Tax and PP2A, respectively. Yeast strain L40 was transformed with plasmids expressing the indicated constructs (BDIKK, LexA DNA-binding domain fused with full-length IKK γ or truncation mutants; AD-PP2Ac and AD-Tax represent VP16 activation domain fusions of the human PP2A catalytic subunit and Tax, respectively). Stable transformants were selected and assayed for relative β -galactosidase activity in chloramphenicol red β -galactosidase units. β -Galactosidase activities of the set of strains containing AD-PP2Ac are represented by solid bars and those containing AD-Tax are represented by open bars. *B*, a yeast three-hybrid assay was used to assess the effect of Tax on PP2A- $\text{IKK}\gamma$ binding. The Tax gene, under the control of the Met-25 promoter, was integrated into the mating locus of the L40 yeast strains. Binding of the indicated BD IKK γ constructs to ADPP2A constructs was then measured in the presence or absence of methionine (*i.e.* without or with Tax, represented by open or solid bars, respectively) as described for *A*. Results in *A* and *B* are means \pm S.E. from triplicate determinations. *C*, summary of the relative strengths of binding between IKK γ constructs and PP2A in the absence or presence of Tax.

human PP2A C subunits are highly homologous, the human PP2A C α expressed here most likely exists as a holoenzyme with the *S. cerevisiae* A and B subunits. The NH₂-terminal helical domains of IKK γ have been shown to be critical for binding IKK α and IKK β (25, 26). This domain may also be important for the integrity of IKK γ structure such that a deletion of IKK γ amino acid residues 1–150 drastically reduced binding to PP2A C α (Fig. 5, *A* and *B*). In aggregate, these data suggest that the region spanning the HLX2 heptad repeat (amino acids 188–253) is critical for PP2A interaction. Importantly, inclusion of the COOH-terminal CCR2 (amino acids 254–303) and LZ (amino acids 304–365) heptad repeats significantly attenuated HLX2 interaction with PP2A (Fig. 5A, BDIKK γ -1–307 and BDIKK γ -1–419, respectively) suggesting that CCR2 and LZ

heptad repeats negatively modulate the accessibility of HLX2 to PP2A.

Tax Enhances PP2A- $\text{IKK}\gamma$ Binding by Interacting with HLX2 and CCR2 Domains—A similar yeast two-hybrid analysis was performed to map the Tax-binding domain in IKK γ . In contrast to the results described above, BD- $\text{IKK}\gamma$ -1–307, which contained both the HLX2 and CCR2 region, was found to bind Tax the strongest, followed by BD- $\text{IKK}\gamma$ -1–253 and BD- $\text{IKK}\gamma$ -1–419 (Fig. 5A, open bars). Weak interaction was detected for BD- $\text{IKK}\gamma$ -1–188, -151–419, and -151–307 (Fig. 5A, open bars). Little or no interaction between Tax and IKK γ -1–86 was found. These results suggest that Tax and PP2A bind to distinct, but overlapping, regions of IKK γ . Here again, the LZ domain exerted a negative influence on Tax- $\text{IKK}\gamma$ binding also, but unlike PP2A- $\text{IKK}\gamma$ interaction, CCR2 increased Tax- $\text{IKK}\gamma$ binding (compare Fig. 5A, BDIKK γ -1–253 and BDIKK γ -1–307, open bars).

We next investigated how Tax affects IKK γ interaction with PP2A. To this end, a yeast three-hybrid system was employed wherein *tax* gene was placed under the control of the Met25 promoter (kindly provided by J. M. Egly; Ref. 28). The Met25-*tax* expression cassette was then integrated into the mating type locus of the respective L40 reporter strains that already harbored AD-PP2A C α and each of the BD- $\text{IKK}\gamma$ constructs. As indicated in Fig. 5B, Tax greatly promoted IKK γ interaction with PP2A C α . Interestingly, in the presence of Tax (methionine starvation), the profile of the affinities of PP2A C α for various IKK γ deletions was skewed toward that of Tax- $\text{IKK}\gamma$ interaction, with IKK γ -1–307 binding PP2A C α the best (compare Figs. 5A and 4B). This skewing of the interaction profile was observed even when methionine was supplemented in the growth media to suppress *tax* expression. The repression of the Met-25 promoter was, however, incomplete, as a low but detectable level of Tax remained (data not shown). The leaky expression of Tax is most likely responsible for the deviation of the Met + IKK γ -PP2A interaction profile in Fig. 5B (open bars) from those in Figs. 4 and Fig. 5A. These results suggest that IKK γ -1–307 contains the domains required for strong Tax- $\text{IKK}\gamma$ -PP2A ternary complex formation. Furthermore, Tax facilitates PP2A binding to IKK γ by a direct interaction with

IKK γ Is a Molecular Switch

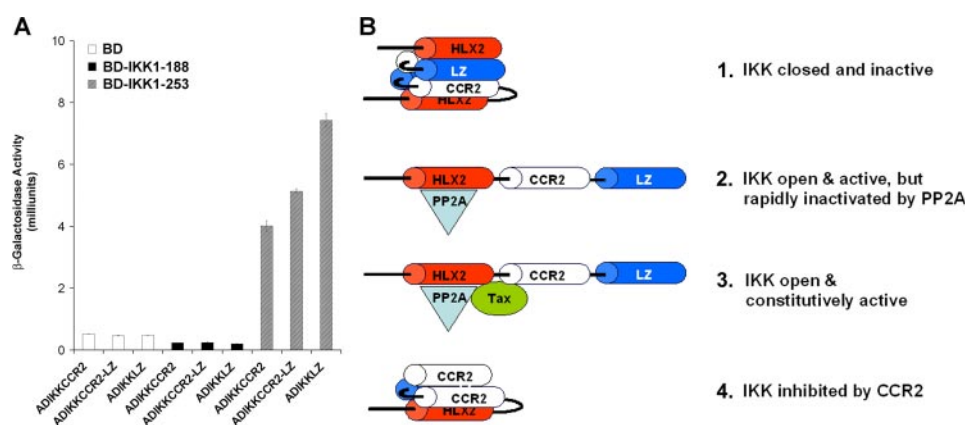


FIGURE 6. CCR2 and LZ heptad repeats directly bind HLX2. *A*, yeast L40 was transformed with plasmids expressing the BD-IKK constructs and various ADIKK constructs that contained the VP16 activation domain fused with CCR2, LZ, and CCR2-LZ, respectively. Stable transformants were selected and assayed for relative β -galactosidase activity as described in the legend to Fig. 5. Results are means \pm S.E. from triplicate determinations. *B*, a model to explain the heptad-repeat interactions that modulate PP2A recruitment and the alteration of the heptad repeat-PP2A interaction by Tax. HLX2, CCR2, and LZ form a helical bundle in which HLX2 is sequestered from binding PP2A. When the HLX2-CCR2-LZ bundle forms, IKK γ is in a closed and inactive conformation (*B1*). In this resting state, it is not necessary for IKK to recruit PP2A and HLX is blocked from PP2A access. The HLX2-CCR2-LZ interaction, however, can become disrupted after Tax binding to HLX2 and CCR2 or by signal (e.g. TNF- α)-induced post-translational modifications. When HLX2-CCR2-LZ bundle is unfolded, IKK γ and IKK assume an open and active conformation, which then recruits PP2A via the exposed HLX2 region for rapid inactivation (*B2*). Tax binds IKK γ and converts HLX2-CCR2-LZ bundle into an active conformation, which recruits PP2A, but Tax-PP2A interaction renders PP2A inactive or less active, thereby maintaining IKK γ and IKK in a constitutively active state (*B3*). CCR2 peptide locks the HLX2-CCR2-LZ bundle in a closed conformation, thereby preventing PP2A and Tax binding and IKK activation (*B4*).

both IKK γ and PP2A and possibly by converting IKK γ into a conformation favorable for PP2A binding. The protein interaction results are summarized in Fig. 5C.

The CCR2 and LZ Domains of IKK γ Interact with HLX2 and Modulate Its Interaction with PP2A and Tax—Because IKK γ truncations lacking the CCR2 and LZ heptad repeats showed greater affinity for PP2A and Tax than the full-length IKK γ , we surmised that CCR2 or LZ might negatively modulate the accessibility of HLX2 to PP2A. Because HLX2, CCR2, and LZ domains are extensively helical, it follows that CCR2 and/or LZ may directly bind HLX2 through intra- or intermolecular coiled-coil interaction, thereby restricting HLX access by PP2A.

To assess the interaction between CCR2 and LZ with HLX2, yeast two-hybrid analysis was again performed. As shown in Fig. 6, both CCR2 and LZ bound IKK γ -1–253 strongly but did not bind the empty vector control or LexA-IKK γ -1–188 at all (Fig. 6A). CCR2-LZ dual heptad repeats also interacted with HLX2 with significant affinity (Fig. 6A, ADIKKCCR2-LZ). Because CCR2 and LZ have been shown to bind each other through coiled-coil interaction (31), and in light of the present results, we think it likely that HLX2, CCR2, and LZ may form a helical bundle in which HLX2 is sequestered from binding PP2A. To extend this line of reasoning further, we hypothesize that when the HLX2-CCR2-LZ bundle forms, IKK γ is in a closed and inactive conformation (Fig. 6B1). In this resting state, it is not necessary for IKK to recruit PP2A and HLX is blocked from PP2A access. The HLX2-CCR2-LZ interaction, however, can become disrupted after Tax binding to HLX2 and CCR2 or by signal (e.g. TNF- α)-induced post-translational modifications. When HLX2-CCR2-LZ bundle is unfolded, IKK γ and IKK assume an open and active conformation, which

then recruits PP2A via the exposed HLX2 region for rapid IKK inactivation (Fig. 6B2). Tax binds IKK γ and converts HLX2-CCR2-LZ bundle into an active conformation, which recruits PP2A, but Tax-PP2A interaction renders PP2A inactive or less active, thereby maintaining IKK γ and IKK in a constitutively active state (Fig. 6B3).

CCR2, LZ, and CCR2-LZ Fusion Potently Inhibit NF- κ B Activation by Tax and TNF- α —To test the hypothesis outlined above, we derived expression vectors for dual HA and VP16 activation domain (HA-VP16)-tagged CCR2, LZ, and CCR2-LZ fusions and co-transfected them individually with Tax, and E-sel-Luc, a luciferase reporter driven by the NF- κ B-responsive E-selectin promoter. Indeed, in the forms of HA-VP16 fusions, CCR2 in particular, followed by LZ and CCR2-LZ, all drastically inhibited Tax-mediated (Fig. 7A) and TNF- α -

induced NF- κ B activation (Fig. 7B) in a dose-dependent manner. After HA-VP16-CCR2 expression plasmid was transfected into 293T cells, a direct binding of CCR2 to IKK γ could be readily detected (Fig. 7C). Finally, CCR2 added *in trans* by transfection reduced IKK γ -Tax and IKK γ -PP2A association in a dose-dependent manner (Fig. 7D, *IP: HA panels, IB: Tax and PP2Ac, respectively*) but did not affect IKK γ -IKK β interaction (Fig. 7D *IP: HA panels, IB: IKK β*). These results support the notion that CCR2, and possibly LZ as well, interacts with HLX2 to form a helical bundle and negatively regulates IKK γ access by PP2A (Fig. 6B4).

DISCUSSION

In this study, we have shown that PP2A holoenzyme interacts with IKK γ . We have further demonstrated that the interaction between PP2A and IKK is tightly controlled. In resting cells, IKK binds PP2A weakly, but upon TNF- α stimulation, IKK undergoes a structural change, possibly as a result of post-translational modifications and/or interaction with other regulatory factors, that facilitates recruitment of PP2A. We have mapped the domains in IKK γ that interact with PP2A and Tax, respectively. As might be expected, the PP2A- and Tax-binding domains in IKK overlap and are localized to amino acid residues 188–253 (HLX2) and 188–307 (HLX2-CCR2), respectively. The latter observation agrees in part with a previous report, which also showed the HLX2 region to be critical for Tax binding (32). The present study has further revealed the importance of HLX2 in binding PP2A and how its interaction with PP2A and Tax is regulated by downstream CCR2 and LZ heptad repeats. Although both CCR2 and LZ negatively control HLX2-PP2A binding, CCR2 is needed for strong HLX2-Tax interaction. In the presence of Tax, the binding between IKK γ

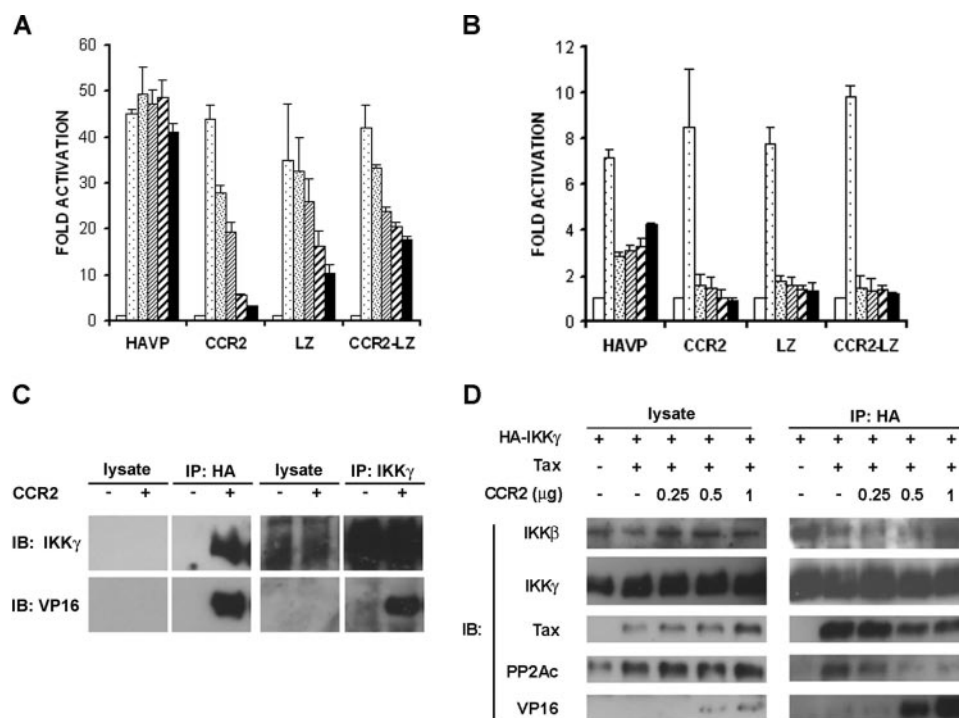


FIGURE 7. CCR2, LZ and CCR2-LZ heptad repeats expressed in trans potentially inhibit NF- κ B activation by TNF- α or Tax and disrupt IKK γ interaction with Tax and PP2A. *A*, CCR2 and LZ heptad repeats block NF- κ B activation by Tax. HEK293T cells were transfected with 1 μ g of E-selectin-Luc, 0.5 μ g of pRL-TK, with or without 0.5 μ g of Tax expression vector and, in increasing concentrations, expression plasmids for HA-VP16 (HAVP) alone or HA-VP16 fusions containing CCR2, LZ, and CCR2-LZ repeats (labeled as CCR2, LZ, and CCR2-LZ, respectively). The open, dotted, densely dotted, hatched, thickly hatched, and solid bars represent without Tax, and Tax plus 0, 0.25, 0.5, 1.0, and 2.0 μ g of HVP, CCR2, LZ, and CCR2-LZ expression plasmids, respectively. The total DNA amount was held constant by the addition of pcDNA3.1. Cells were harvested for luciferase assays 48 h after transfection. *B*, CCR2 and LZ heptad repeats block NF- κ B activation by TNF- α . HEK293T cells were transfected as described for *A* except that the Tax expression construct was not included. Forty hours post-transfection, human TNF- α (2 ng/ml) was added and incubated for 8 h. Cells were harvested at the end of the TNF- α treatment for luciferase assays. Results in *A* and *B* are means \pm S.E. from triplicate determinations. *C*, CCR2 binds IKK γ *in vivo*. HEK293T cells were transiently transfected with 2 μ g of pcDNA or pcDNA-HAVP-CCR2, respectively. Cells were harvested 48 h post-transfection and immunoprecipitated with HA antibody-conjugated agarose or an anti-IKK γ antibody followed by protein G pull-down. IKK γ and CCR2 were detected by anti-IKK γ (*IB*: IKK γ) and anti-VP16 (*IB*: VP16) antibodies, respectively. *D*, CCR2 disrupts PP2A and Tax binding to IKK γ . HEK293T cells were transiently transfected with 0.5 μ g of pcDNA-HA-IKK γ , 1.5 μ g of CMV-Tax, and increasing amounts (0.25, 0.5, and 1 μ g) of pcDNA-HAVP-CCR2. Cells were harvested 48 h post-transfection and immunoprecipitated with HA antibody-conjugated agarose. IKK β , IKK γ , Tax, PP2Ac, and CCR2 were detected by immunoblots (*IB*) with appropriate antibodies. The left and right panels represent immunoblots for the whole cell lysates (*lysate*) and those of HA-IKK γ immunoprecipitates (*IP: HA*), respectively.

and PP2A became greatly increased, consistent with our published results that Tax, PP2A, and IKK form a stable ternary complex (16).

What is particularly interesting is that the CCR2, LZ, and CCR2-LZ fusion bind HLX2 directly and negatively affect HLX2 access by PP2A and Tax. The propensity for HLX2 to form coiled coil is predicted to be lower than that for CCR2 and LZ (20% versus 90–100% based on the multicoil program; Ref. 29). This may be due in part to its critical role in dynamic interactions with multiple protein partners, wherein a flexible and less structured motif is more desirable. Remarkably, CCR2, LZ, and CCR2-LZ fusion potentially inhibited NF- κ B activation by Tax and TNF- α , and CCR2 disrupted PP2A and Tax binding with IKK γ . Based on these results, we hypothesize that, in its resting/inactive state, CCR2 and LZ heptad repeats may interact with HLX2 in a helical bundle and sequester HLX2 from access by PP2A. When IKK becomes activated, HLX2 assumes an open conformation, which

avidly and rapidly recruits PP2A to turn off IKK activity. This open form of IKK γ is stabilized or induced by Tax. The HLX2 region of the Tax-associated IKK γ is exposed and avidly recruits PP2A. However, the interaction between Tax and PP2A inhibits PP2A activity and prevents PP2A from inactivating IKK. The current data do not rule out the possibility that CCR2, LZ and CCR2-LZ fusion peptides may also affect intermolecular IKK γ interaction (oligomerization), thereby affecting Tax-PP2A binding. Detailed biochemical analyses using purified components are currently in progress to address this issue. Finally, a recent study has indicated that the CCR2-LZ region of IKK γ contains a K63-polyubiquitin-binding domain and its interaction with K63-polyubiquitin is required for IKK activation (33). It is possible that binding of K63-polyubiquitin to CCR2-LZ also alters IKK γ and IKK structures in a manner similar to Tax-CCR2-HLX2 interaction and thereby induces IKK to assume an open conformation.

It has been reported recently that a deletion of amino residues 121–179 of IKK γ prevented PP2A recruitment by IKK γ and attenuated IKK activity (34). In the same study, okadaic acid, a PP2A inhibitor, was found to attenuate TNF- α induced degradation of I κ B (34). These data were taken to suggest

that IKK γ -121–179 constitutes the PP2A-binding domain, and PP2A plays a positive role in IKK activation (34). The major PP2A-binding domain of IKK γ that we have mapped is localized to the HLX2 region in residues 189–253 and differs from the previous report. In our analyses, even though the COOH-truncation mutant IKK γ -1–188 did bind PP2A somewhat, its extent of binding is negligible compared with that of the HLX2-containing IKK γ -1–253. The fact that Tax-enhanced PP2A binding was observed for IKK γ -1–253 but not for IKK γ -1–188, again, supports the notion that HLX2 is the bona fide PP2A-binding site. It is possible that the loss of PP2A binding from the IKK γ -121–179 deletion may have resulted in a structural disruption to the coiled-coil region 1 of IKK γ , which secondarily affected the conformation of HLX2. Whether PP2A plays a negative, positive, or dual role in regulating IKK activity also remains to be fully resolved. Okadaic acid, a PP2A inhibitor, has been shown by multiple investigators to potentially activate IKK and I- κ B degradation (14, 15). Published literature suggests that

once IKK is activated by T-loop phosphorylation, it undergoes further hyperphosphorylation and becomes attenuated in its activity. PP2A may play a role in removing all phosphate moieties from IKK, thereby returning IKK to its fully resting state, or perhaps under some circumstances, removing only the inhibitory phosphates while leaving the activating phosphate intact. Although the IKK activity of Tax-IKK-PP2A complex appears constitutively active as judged by the constant phosphorylation and total destruction of I- κ B in Tax-expressing cells, the status of IKK phosphorylation in the complex is unclear. It is possible that under the influence of Tax, a spectrum of T-loop-phosphorylated and hyperphosphorylated forms of IKK are represented. The data reported here do not rule out a positive role of PP2A in IKK activation.

The exact nature of the putative helical bundle formed by HLX2-CCR2-LZ is not clear at present. Several reports have already suggested a similarity between CCR2-LZ of IKK γ to the helical domains in HIV gp41, influenza virus HA2, and other viral fusion proteins (31, 35). The heptad repeats of gp41 and HA2 alternate between a six-helical bundle formed by trimeric α -helical hairpins and three fully extended α -helices to facilitate fusion peptide insertion into target cell membrane and subsequent viral and host cell membrane fusion. It has been proposed recently that the stoichiometry of IKK holoenzyme is $\alpha_1\beta_1\gamma_2$ or $\beta_2\gamma_2$, with each IKK holoenzyme containing two IKK γ subunits (8). Based on the results above, we speculate that the HLX2, CCR2, and LZ heptad repeats of the two IKK γ subunits may also alternate between a six-helix bundle and two fully extended helices as a function of post-translational modifications or interaction with K63-polyubiquitin or with HTLV-1 Tax (Fig. 6B). Additional helical interactions between the fully extended helices may maintain IKK in ($\beta_2\gamma_2$) or ($\beta_2\gamma_2$)₂ structure and allow IKK catalytic subunits to undergo auto-phosphorylation and activation. Finally, in light of the recent success of HIV fusion inhibitors, the activity of IKK and NF- κ B may also be modulated using peptides with sequences spanning HLX2, CCR2, and LZ heptad repeats as reported here and elsewhere (23).

Acknowledgments—We thank Dr. K. T. Jeang for the human IKK γ expression construct, Dr. J. M. Egly for the Met25-plasmid, and Dr. G. Walter for the expression plasmids for the PP2A B subunits.

REFERENCES

- Hayden, M. S., and Ghosh, S. (2004) *Genes Dev.* **18**, 2195–2224
- Ghosh, S., and Karin, M. (2002) *Cell* **109**, (suppl.) S81–S96
- Cheong, R., Bergmann, A., Werner, S. L., Regal, J., Hoffmann, A., and Levchenko, A. (2006) *J. Biol. Chem.* **281**, 2945–2950
- Werner, S. L., Barken, D., and Hoffmann, A. (2005) *Science* **309**, 1857–1861
- Yamaoka, S., Courtois, G., Bessia, C., Whiteside, S. T., Weil, R., Agou, F., Kirk, H. E., Kay, R. J., and Israel, A. (1998) *Cell* **93**, 1231–1240
- Karin, M., and Ben Neriah, Y. L. (2000) *Annu. Rev. Immunol.* **18**, 621–663

- DiDonato, J. A., Hayakawa, M., Rothwarf, D. M., Zandi, E., and Karin, M. (1997) *Nature* **388**, 548–554
- Miller, B. S., and Zandi, E. (2001) *J. Biol. Chem.* **276**, 36320–36326
- Tegethoff, S., Behlke, J., and Scheidereit, C. (2003) *Mol. Cell. Biol.* **23**, 2029–2041
- Yin, M. J., Christerson, L. B., Yamamoto, Y., Kwak, Y. T., Xu, S., Mercurio, F., Barbosa, M., Cobb, M. H., and Gaynor, R. B. (1998) *Cell* **93**, 875–884
- Wang, C., Deng, L., Hong, M., Akkaraju, G. R., Inoue, J., and Chen, Z. J. (2001) *Nature* **412**, 346–351
- Sun, L., Deng, L., Ea, C. K., Xia, Z. P., and Chen, Z. J. (2004) *Mol. Cell* **14**, 289–301
- Ea, C. K., Sun, L., Inoue, J., and Chen, Z. J. (2004) *Proc. Natl. Acad. Sci. U. S. A.* **101**, 15318–15323
- Sung, S. J., Walters, J. A., and Fu, S. M. (1992) *J. Exp. Med.* **176**, 897–901
- Schmidt, K. N., Traenckner, E. B., Meier, B., and Baeuerle, P. A. (1995) *J. Biol. Chem.* **270**, 27136–27142
- Fu, D. X., Kuo, Y. L., Liu, B. Y., Jeang, K. T., and Giam, C. Z. (2003) *J. Biol. Chem.* **278**, 1487–1493
- Sun, S. C., Elwood, J., Beraud, C., and Greene, W. C. (1994) *Mol. Cell. Biol.* **14**, 7377–7384
- Good, L., and Sun, S. C. (1996) *J. Virol.* **70**, 2730–2735
- Sun, S. C., and Ballard, D. W. (1999) *Oncogene* **18**, 6948–6958
- Xiao, G., and Sun, S. C. (2000) *Oncogene* **19**, 5198–5203
- Chu, Z. L., Di Donato, J. A., Hawiger, J., and Ballard, D. W. (1998) *J. Biol. Chem.* **273**, 15891–15894
- Chu, Z. L., Shin, Y. A., Yang, J. M., Di Donato, J. A., and Ballard, D. W. (1999) *J. Biol. Chem.* **274**, 15297–15300
- Agou, F., Courtois, G., Chiaravalli, J., Baleux, F., Coic, Y. M., Traincard, F., Israel, A., and Veron, M. (2004) *J. Biol. Chem.* **279**, 54248–54257
- Jin, D. Y., Giordano, V., Kibler, K. V., Nakano, H., and Jeang, K. T. L. H. (1999) *J. Biol. Chem.* **274**, 17402–17405
- May, M. J., Marienfeld, R. B., and Ghosh, S. (2002) *J. Biol. Chem.* **277**, 45992–46000
- May, M. J., D'Acquisto, F., Madge, L. A., Glockner, J., Pober, J. S., and Ghosh, S. (2000) *Science* **289**, 1550–1554
- Hollenberg, S. M., Sternglanz, R., Cheng, P. F., and Weintraub, H. (1995) *Mol. Cell. Biol.* **15**, 3813–3822
- Tirode, F., Malaguti, C., Romero, F., Attar, R., Camonis, J., and Egly, J. M. (1997) *J. Biol. Chem.* **272**, 22995–22999
- McDonnell, A. V., Jiang, T., Keating, A. E., and Berger, B. (2006) *Bioinformatics* **22**, 356–358
- Shih, H. M., Goldman, P. S., De Maggio, A. J., Hollenberg, S. M., Goodman, R. H., and Hoekstra, M. F. (1996) *Proc. Natl. Acad. Sci. U. S. A.* **93**, 13896–13901
- Agou, F., Traincard, F., Vinolo, E., Courtois, G., Yamaoka, S., Israel, A., and Veron, M. (2004) *J. Biol. Chem.* **279**, 27861–27869
- Iha, H., Kibler, K. V., Yedavalli, V. R., Peloponese, J. M., Haller, K., Miyazato, A., Kasai, T., and Jeang, K. T. (2003) *Oncogene* **22**, 8912–8923
- Ea, C. K., Deng, L., Xia, Z. P., Pineda, G., and Chen, Z. J. (2006) *Mol. Cell* **22**, 245–257
- Kray, A. E., Carter, R. S., Pennington, K. N., Gomez, R. J., Sanders, L. E., Llanes, J. M., Khan, W. N., Ballard, D. W., and Wadzinski, B. E. (2005) *J. Biol. Chem.* **280**, 35974–35982
- Filipe-Santos, O., Bustamante, J., Haverkamp, M. H., Vinolo, E., Ku, C. L., Puel, A., Frucht, D. M., Christel, K., von Bernuth, H., Jouanguy, E., Feinberg, J., Durandy, A., Senechal, B., Chapgier, A., Vogt, G., de Beaucoudrey, L., Fieschi, C., Picard, C., Garfa, M., Chemli, J., Bejaoui, M., Tsolia, M. N., Kutukculer, N., Plebani, A., Notarangelo, L., Bodemer, C., Geissmann, F., Israel, A., Veron, M., Knackstedt, M., Barbouche, R., Abel, L., Magdorf, K., Gendrel, D., Agou, F., Holland, S. M., and Casanova, J. L. (2006) *J. Exp. Med.* **203**, 1745–1759